Studies of the $\mathbf{k}_\perp$–dependence in uPDFs

Analysis center studentship 08/30/2010 to 10/08/2010: final writeup

Henning Sedello

email: `henning.sedello@tu-dortmund.de`

10/21/2010

Summary: During the studentship Gaussian (normal) parametrizations of the uPDFs' $k_\perp$ dependence are compared to measurements of inclusive dijet events at Hera. It is found that for a fixed width of 1 GeV a vanishing or small mean in the distribution is favored.

1 Introduction

Unintegrated parton density functions (uPDFs) are part of the CCFM[1, 2, 3, 4] description of high energy scattering processes of hadrons. An introduction to this theory can for example be found in [5, 6], and in the references therein. Also notations not explicitly defined here may be found in these references.

Events generated with Gaussian parametrizations of the uPDFs' $k_\perp$ dependence are in the following compared to measured inclusive dijet events in e^+p collisions at the Hera collider ($E_{e^+} = 27.5\,\mathrm{GeV}$, $E_P = 820\,\mathrm{GeV}$) published by the H1 collaboration[7].

2 Simulation steps

The simulation of dijet events given an uPDF starting parametrization can be divided in the following computational task:

1. Calculate the CCFM evolution kernel using the Monte Carlo (MC) program SMALLX[8]. Store the kernel as a grid in the file `test-grid.dat`. (Input parameters: Figure 8)

2. Use the kernel to generate a grid for $\mathcal{A}(x, \bar{q}, k_\perp)$. (CALCGLUE[9]) Results are stored in the file `ccfm-test.dat`

3. Generate hadron level events with CASCADE 2.2.0[6], populate histograms with the HZTOOL-4.3[10] subroutine `hz03160`.

4. Compare MC to data distributions via the χ^2 statistic defined below to assess the data's sensitivity to the parametrization.

Definition of the χ^2 statistic used:

$$\chi^2 = \sum_{n=0}^{N} \frac{\left(Y_{\text{data}}^{(n)} - Y_{\text{MC}}^{(n)}\right)^2}{\left(\delta Y_{\text{data}}^{(n)}\right)^2 + \left(\delta Y_{\text{MC}}^{(n)}\right)^2} \tag{1}$$

With

$Y_{\text{data/MC}}^{(n)}$	:	Content of bin n of the data or MC histogram
$\delta Y_{\text{data}}^{(n)}$	:	Total error of bin n of the data histogram
$\delta Y_{\text{MC}}^{(n)}$	:	Total error of bin n of the MC histogram
N	:	Number of bins

3 Inspected dijet distributions

While various distributions of dijet events are published in [7], the focus here is on two distributions which are potentially sensitive to the gluon $k_\perp$ distribution:

1. The inclusive dijet cross section multiplied by $\langle x \rangle$, averaged over x and Q^2 in dependence of Δ (Figure 2 in [7]).

2. The fraction $S(120)$ of events where the two hardest jets open an azimuthal angle less than 120° (Figure 9 in [7]) in dependence on x. Explicitly S is defined as

$$S(\alpha) = \frac{\int_0^\alpha N_{\text{dijet}}(\Delta\phi^*, x, Q^2)\mathrm{d}\Delta\phi^*}{\int_0^{180^\circ} N_{\text{dijet}}(\Delta\phi^*, x, Q^2)\mathrm{d}\Delta\phi^*}. \tag{2}$$

4 uPDF starting parametrization—Gaussian for $\mathbf{k}_\perp$

The uPDF starting parametrization is split into an x dependent part, implemented in CALCGLUE, and a $k_\perp$ starting distribution, implemented in SMALLX. The following distributions are used here:

- The x starting distribution is chosen according to a recent fit to F_2 data[11],

$$A_0(x) = N x^{-B}(1-x)^C(1-Dx) \qquad \text{with} \qquad \begin{array}{rcl} N & = & 0.417 \\ B & = & 0.125 \\ C & = & 4.0 \\ D & = & -9.2 \end{array} \tag{3}$$

  (See Figure 9 for the modifications applied to `calcglu.F`.)

- The probability density for generating the starting $k_\perp$ values in SMALLX is a Gaussian distribution in $k_\perp$, *i.e.*

$$\mathcal{P}(k_\perp) = \frac{1}{\sqrt{2\pi\sigma^2}} \mathrm{e}^{-\frac{(k_\perp - \mu)^2}{2\sigma^2}}. \tag{4}$$

  (See Figure 6 for the modifications applied to `sminfn_gluon.f`.)

For the two parameters μ and σ the following one–dimensional χ^2 scans are performed.

4.1 χ^2 scan: μ varied, σ fixed

For μ in the range $0.12 - 12.0\,\mathrm{GeV}$ and $\sigma = 1\,\mathrm{GeV}$, per parameter point 10.000.000 events are generated with SMALLX and 5.000.000 with CASCADE.

χ^2/N is shown in Figure 1 for both distributions described in section 3. For the parameter points highlighted in Figure 1, the distributions of [7] enlisted in section 3 are reproduced in Figure 4.

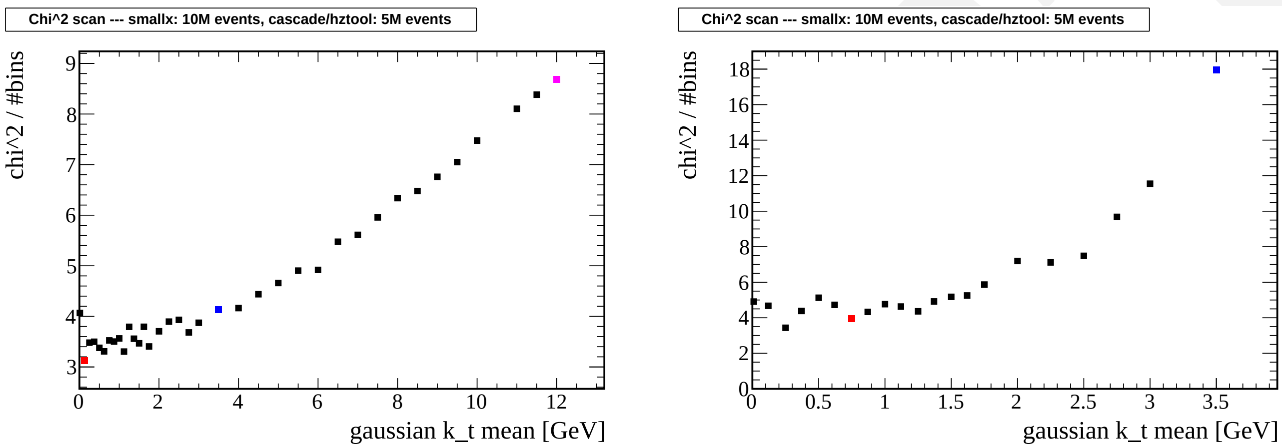

(a) χ^2 scan for the distributions of Figure 2 of [7]

(b) χ^2 scan for the distributions of Figure 9 in [7]

Figure 1: χ^2 scans: Generated with 10.000.000 events in SMALLX and 5.000.000 events in CASCADE. The colored dots mark the Monte Carlo distributions in Figures 4.

Obviously, the best description of the data examined is given by small values of μ.

4.2 χ^2 scan: μ fixed, σ varied

For $\mu = 0\,\mathrm{GeV}$ and σ in the range $0.25 - 4\,\mathrm{GeV}$, 10.000.000 events are generated with SMALLX and 5.000.000 with CASCADE per parameter point.

χ^2/N is shown in Figure 2 for both distributions described in section 3. The distributions of [7] are reproduced in Figure 5 for the parameter points highlighted in Figure 2.

As can be seen in Figure 5, the program chain failed to produce realistic events for $\mu = 0\,\mathrm{GeV}$ and small means ($\sigma = 0.25\,\mathrm{GeV}$). This is probably due to the collinear cutoff[6] Q_0, which was chosen here to be $Q_0 = 1.3\,\mathrm{GeV}$, see the listing in Figure 8.

The distribution of $S(120°)$ in Figure 5a seems to favor $\sigma \lesssim \mathcal{O}(1\,\mathrm{GeV})$, as even the MC distribution for $\sigma = 1.25\,\mathrm{GeV}$ overshoots the data. However, this enhancement as well as the rather flat distribution for $0.75\,\mathrm{GeV} \leq \sigma \leq 1.5\,\mathrm{GeV}$ in Figure 2 can probably be explained with the large cutoff Q_0.

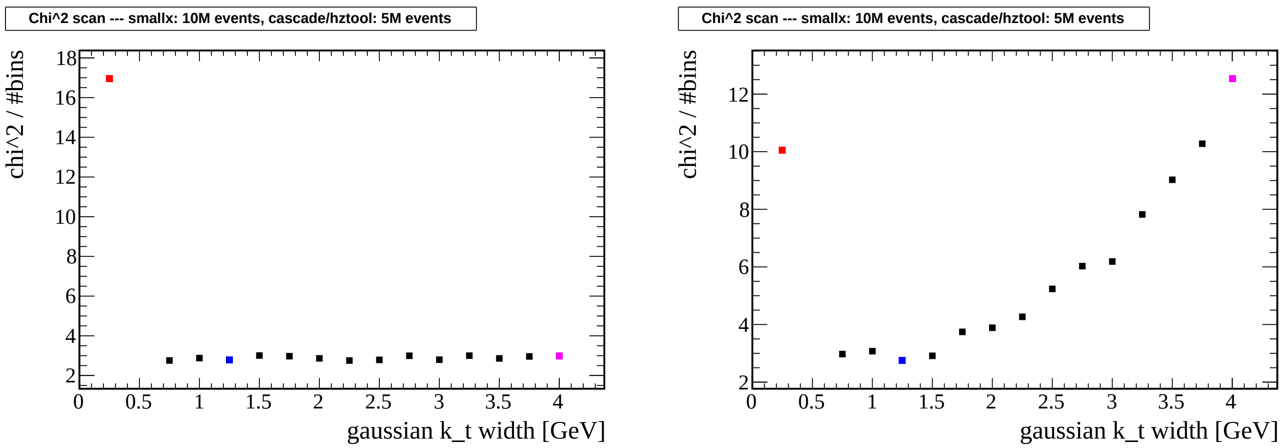

(a) χ^2 scan for the distributions of Figure 2 of [7]

(b) χ^2 scan for the distributions of Figure 9 in [7]

Figure 2: χ^2 scans: Generated with 10.000.000 events in SMALLX and 5.000.000 events in CASCADE. The colored dots mark the MC distributions in Figures 5.

5 uPDF starting parametrization—Gaussian for $\mathbf{k}_\perp{}^2$

As a variation, a Gaussian distribution in $k_\perp^2$ is examined, *i.e.*

$$\mathcal{P}(k_\perp^2) = \frac{1}{\sqrt{2\pi\sigma^2}} \mathrm{e}^{-\frac{(k_\perp^2-\mu)^2}{2\sigma^2}}. \tag{5}$$

(See Figure 7 for the modifications applied to `sminfn_gluon.f`.)

A χ^2 scan has been performed for $\sqrt{\mu}$ in $0.01 - 3.5\,\mathrm{GeV}$ and $\sqrt{\sigma} = 1\,\mathrm{GeV}$ with 10.000.000 events in SMALLX and 5.000.000 events in CASCADE. The numeric results are depicted in Figure 3 for both distributions of section 3.

6 Acknowledgements

I like to thank Albert Knutsson of the Terascale Monte Carlo group at DESY Hamburg for his friendly and professional supervision. Further I like to thank Hannes Jung for the discussions on CCFM and his program codes, and Thomas Schörner–Sadenius for the organization of the studentship.

The Analysis Center Studentship is financed by the Helmholtz Alliance "Physics at the Terascale".

References

[1] M. Ciafaloni, "Coherence Effects in Initial Jets at Small q**2 / s," *Nucl. Phys.* **B296** (1988) 49.

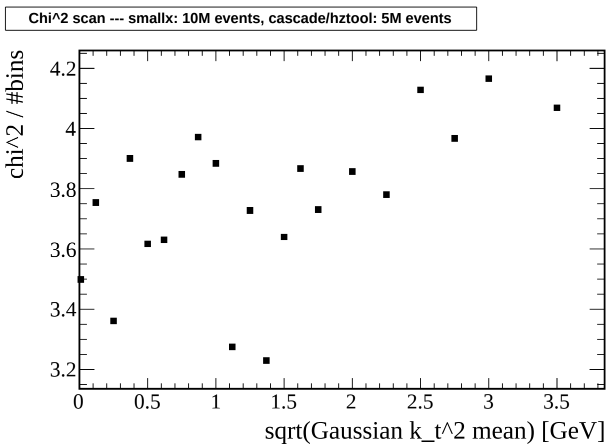

(a) χ^2 scan for the distributions of Figure 2 of [7]

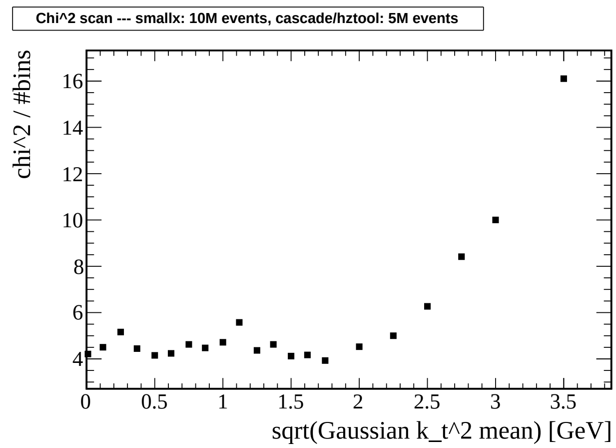

(b) χ^2 scan for the distributions of Figure 9 in [7]

Figure 3: χ^2 scans: Generated with 10.000.000 events in SMALLX and 5.000.000 events in CASCADE.

[2] S. Catani, F. Fiorani, and G. Marchesini, "QCD Coherence in Initial State Radiation," *Phys. Lett.* **B234** (1990) 339.

[3] S. Catani, F. Fiorani, and G. Marchesini, "Small x Behavior of Initial State Radiation in Perturbative QCD," *Nucl. Phys.* **B336** (1990) 18.

[4] G. Marchesini, "QCD coherence in the structure function and associated distributions at small x," *Nucl. Phys.* **B445** (1995) 49–80, `arXiv:hep-ph/9412327`.

[5] **Small x** Collaboration, B. Andersson *et al.*, "Small x phenomenology: Summary and status," *Eur. Phys. J.* **C25** (2002) 77–101, `arXiv:hep-ph/0204115`.

[6] H. Jung *et al.*, "The CCFM Monte Carlo generator CASCADE 2.2.0," `arXiv:1008.0152 [hep-ph]`.

[7] **H1** Collaboration, A. Aktas *et al.*, "Inclusive dijet production at low Bjorken-x in deep inelastic scattering," *Eur. Phys. J.* **C33** (2004) 477–493, `arXiv:hep-ex/0310019`.

[8] H. Jung, "ccfm grid source." via email on 09/12/2010.

[9] H. Jung, "calcglu changes for cascade." via email on 09/12/2010.

[10] J. Bromley *et al.*, "HZTOOL: A package for Monte Carlo-data comparison at HERA (version 1.0),". Prepared for Workshop on Future Physics at HERA (Preceded by meetings 25-26 Sep 1995 and 7-9 Feb 1996 at DESY), Hamburg, Germany, 30-31 May 1996.

[11] A. Bacchetta, H. Jung, A. Knutsson, K. Kutak, and F. von Samson-Himmelstjerna, "A method for tuning parameters of Monte Carlo generators and a determination of the unintegrated gluon density," `arXiv:1001.4675 [hep-ph]`. (accepted for Eur. Phys. J.).

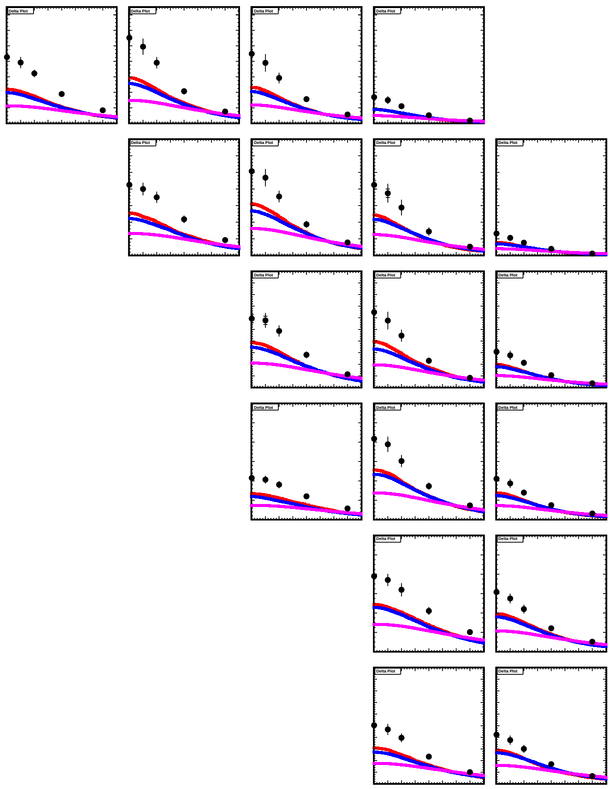

(a) $x\frac{\mathrm{d}^2\sigma}{\mathrm{d}Q^2\mathrm{d}x}$ $(\frac{\mathrm{pb}}{\mathrm{GeV}^2})$ vs Δ (GeV)

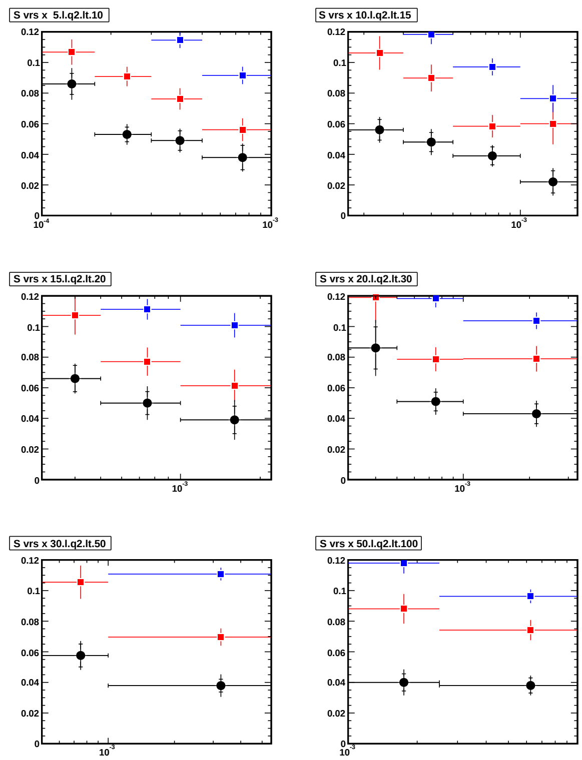

(b) $S(120°)$ vs x

Figure 4: Figures corresponding to Figures 2 and 9 of [7]. Black: data, colored: MC samples from the scan (see Figure 1). The ranges of the axes are chosen in accordance with the original figures (up to the factor of 10^{-3} in the x axis of (b)).

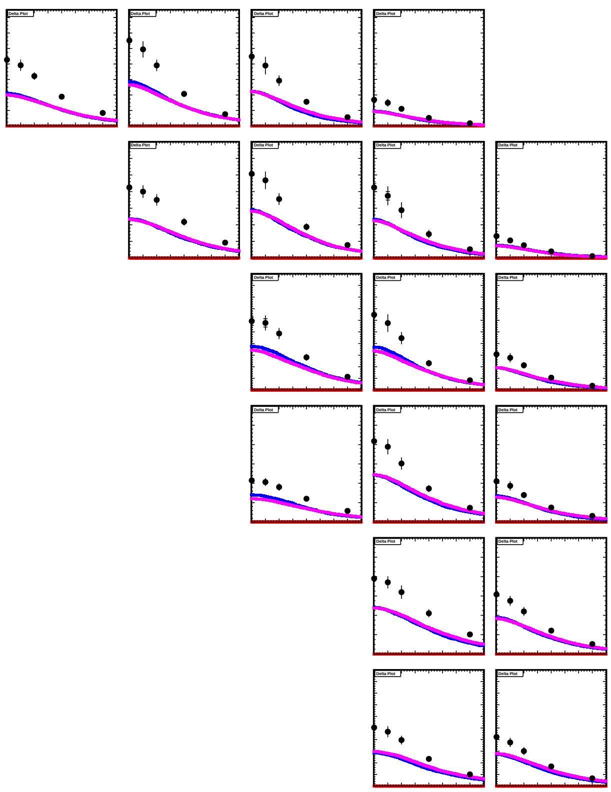

(a) $x\frac{\mathrm{d}^2\sigma}{\mathrm{d}Q^2\mathrm{d}x}$ $(\frac{\mathrm{pb}}{\mathrm{GeV}^2})$ vs Δ (GeV)

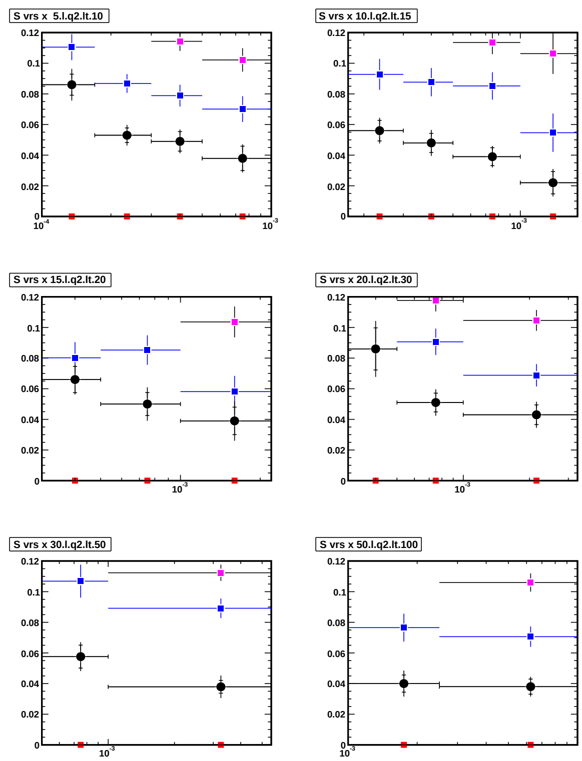

(b) $S(120°)$ vs x

Figure 5: Figures corresponding to Figures 2 and 9 of [7]. Black: data, colored: MC samples from the scan (see Figure 2). The ranges of the axes are chosen in accordance with the original figures (up to the factor of 10^{-3} in the x axis of (b)).

```
43,44c43,44
<
<       Double Precision sigm, xmean
---
>       Double Precision sigmin, xmeanin, hskt, hsphi
>       common /gaussalb/sigmin,xmeanin
84,90c84,87
<           P(1,0)= SMrgau(1,0.0d0,Qx)
<           P(2,0)= SMrgau(2,0.0d0,Qx)
< c new test for Albert
< c         sigm = 3.0/sqrt(2.)
< c          xmean = 3.
< c          P(1,0)= SMrgau(1,xmean,sigm)
< c          P(2,0)= SMrgau(2,xmean,sigm)
---
>           hskt= SMrgau(1,xmeanin,sigmin)
>           hsphi=2*acos(-1.)*SMRGEN(I)
>           P(1,0)= hskt*sin(hsphi)
>           P(2,0)= hskt*cos(hsphi)
```

Figure 6: Modifications applied to `sminfn_gluon.f`[8] in `.diff` format—Gaussian $k_\perp$

```
43,44c43,44
<
<       Double Precision sigm, xmean
---
>       Double Precision sigmin, xmeanin, hskt, hskt2, hsphi
>       common /gaussalb/sigmin,xmeanin
84,85d83
<           P(1,0)= SMrgau(1,0.0d0,Qx)
<           P(2,0)= SMrgau(2,0.0d0,Qx)
89,90c87,91
< c          P(1,0)= SMrgau(1,xmean,sigm)
< c          P(2,0)= SMrgau(2,xmean,sigm)
---
>           hskt2= SMrgau(1,xmeanin**2,sigmin**2) !absolute value?
>           hskt=sqrt(abs(hskt2))
>           hsphi=2*acos(-1.)*SMRGEN(I)
>           P(1,0)= hskt*sin(hsphi)
>           P(2,0)= hskt*cos(hsphi)
```

Figure 7: Modifications applied to `sminfn_gluon.f`[8] in `.diff` format—Gaussian $k_\perp^2$.

```
Ipgg = 1
ns =  1
Qg = 1.3
Qs = 1.3
Xnorm = 1.
oneLoop = 0
Iglu = 1
```

Figure 8: SMALLX steering input.

```
659,662c659,662
<       A1 = 0.49
<       A2 = 0
<       A3 = 4.9
<       A4 = 0.
---
>         A1=0.417
>         A2=0.125
>         A3=4.0
>         A4=-9.2
672c672,673
<          else
---
>         else
>            test = A1 * 1./x0**A2 * (1.-x0)**A3 * (1.-A4*x0)*xpqs(0)/x0
674d674
<          test =A1*5.*(1./x0**A2)*(1-x0)**A3*(1.-A4*x0)*xpqs(0)/x0
```

Figure 9: Modifications applied to `calcglu.F`[9] in `.diff` format